Correlations between magnetic anomalies and surface geology antipodal to lunar impact basins

N. C. Richmond,[1] L. L. Hood,[2] D. L. Mitchell,[3] R. P. Lin,[4] M. H. Acuña,[5] and A. B. Binder[6]

Received 18 January 2005; revised 1 March 2005; accepted 11 April 2005; published 28 May 2005.

[1] Previous work has shown that the strongest concentrations of lunar crustal magnetic anomalies are located antipodal to four large, similarly aged impact basins (Orientale, Serenitatis, Imbrium, and Crisium). Here, we report results of a correlation study between magnetic anomaly clusters and geology in areas antipodal to Imbrium, Orientale, and Crisium. Unusual geologic terranes, interpreted to be of seismic or ejecta origin associated with the antipodal basins, have been mapped antipodal to both Orientale and Imbrium. All three antipode regions have many high-albedo swirl markings. Results indicate that both of the unusual antipode terranes and Mare Ingenii (antipodal to Imbrium) show a correlation with high-magnitude crustal magnetic anomalies. A statistical correlation between all geologic units and regions of medium to high magnetization when high-albedo features are present (antipodal to Orientale) may suggest a deep, possibly seismic origin to the anomalies. However, previous studies have provided strong evidence that basin ejecta units are the most likely sources of lunar crustal anomalies, and there is currently insufficient evidence to differentiate between an ejecta or seismic origin for the antipodal anomalies. Results indicate a strong correlation between the high-albedo markings and regions of high magnetization for the Imbrium, Orientale, and Crisium antipodes. Combined with growing evidence for an Imbrian age to the magnetic anomalies, this supports a solar wind deflection origin for the lunar swirls.

Citation: Richmond, N. C., L. L. Hood, D. L. Mitchell, R. P. Lin, M. H. Acuña, and A. B. Binder (2005), Correlations between magnetic anomalies and surface geology antipodal to lunar impact basins, *J. Geophys. Res.*, *110*, E05011, doi:10.1029/2005JE002405.

1. Introduction

[2] Magnetic anomaly clusters have been mapped on the Moon at locations antipodal to the similarly aged Orientale, Imbrium, Serenitatis and Crisium impact basins [e.g., *Lin et al.*, 1988]; see Figure 1. One proposed explanation for these anomalies is that they result from magnetization of the antipodal regions in the presence of an amplified magnetic field. An amplified field could result from a plasma cloud generated by the basin forming impact interacting with a weak magnetic field present at the Moon at the time of basin formation [*Hood and Vickery*, 1984; *Hood*, 1987; *Hood and Huang*, 1991]. Impact generated plasma clouds have been observed in laboratory studies [e.g., *Crawford and Schultz*, 1993, 1999]. A second proposed explanation is a cometary collision [*Gold and Soter*, 1976; *Schultz and Srnka*, 1980], where the magnetization results from shock magnetization during the impact of the nucleus in the presence of enhanced field strengths due to the ionized cometary impact. In the latter model, the correlation of magnetic anomaly clusters with basin antipodes is regarded as fortuitous.

[3] High-albedo swirl-like markings have been observed antipodal to Imbrium (Figure 2a), Orientale (Figure 2b), and Crisium (Figure 2c). Similar features have been mapped in other locations, most notably Reiner Gamma in western Oceanus Procellarum (e.g., Lunar Orbiter IV Frame 157 H1). Magnetic shielding of the lunar regolith [*Hood and Schubert*, 1980], a recent impact by a cometary coma [*Schultz and Srnka*, 1980] and surface scouring by recent meteoroid swarms [*Starukhina and Shkuratov*, 2004] have all been proposed as possible explanations for the lunar swirls. *Hood and Schubert* [1980] suggested that the magnetic anomalies would be capable of deflecting the solar wind and could prevent the lunar regolith from reaching optical maturity. Model calculations have indicated that for likely surface fields associated with the strongest lunar anomalies there should be significant deflection of the ion bombardment, resulting in local shielded areas [e.g., *Hood and Williams*, 1989; *Harnett and Winglee*, 2003]. The Lunar

[1]Institute of Geophysics and Planetary Physics, Scripps Institution of Oceanography, University of California, San Diego, La Jolla, California, USA.
[2]Lunar and Planetary Laboratory, University of Arizona, Tucson, Arizona, USA.
[3]Space Science Laboratory, University of California, Berkeley, California, USA.
[4]Space Science Laboratory and Physics Department, University of California, Berkeley, California, USA.
[5]NASA Goddard Space Flight Center, Greenbelt, Maryland, USA.
[6]Lunar Research Institute, Tucson, Arizona, USA.

0148-0227/05/2005JE002405

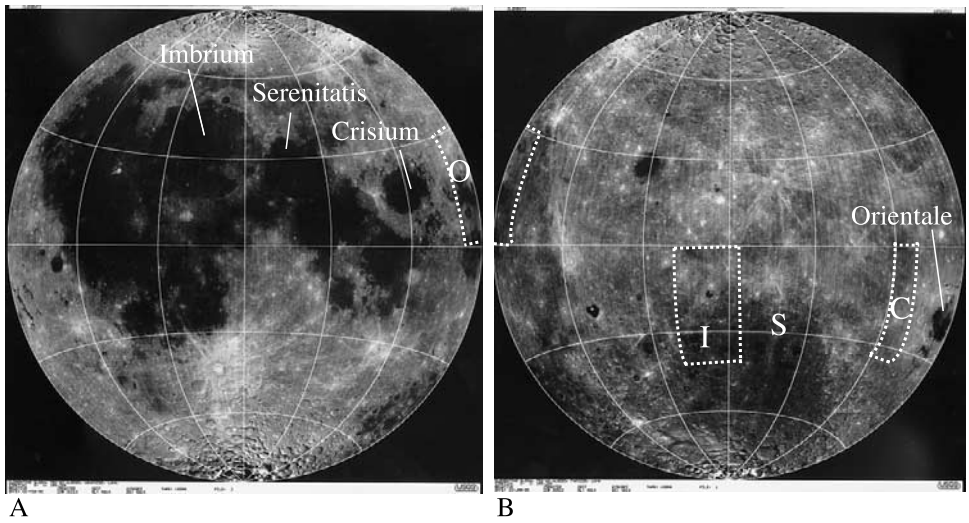

Figure 1. Location of the four large Imbrian-aged basins on the (a) nearside and (b) far side. Antipode positions are labeled I (Imbrium), O (Orientale), C (Crisium), and S (Serenitatis). Boxes correspond to the approximate areas plotted in Figures 3, 5, and 7. Lunar images are from the Clementine albedo map.

Prospector electron reflectometer and magnetometer data sets have shown that the Imbrium antipode fields are strong enough to deflect the solar wind to form a minimagnetosphere one hundred to several hundred kilometers across [*Lin et al.*, 1998]. In contrast, the cometary impact origin argues that the high-albedo swirls are young deposits, remnants of collisions with gas/dust-rich regions within a cometary coma [*Schultz and Srnka*, 1980]. A growing number of studies have indicated a correlation between magnetic anomalies and high-albedo markings [e.g., *Hood*, 1980; *Hood and Williams*, 1989; *Richmond et al.*, 2003], indicating a possible link between the two. Currently, the meteoroid origin to the swirls [*Starukhina and Shkuratov*, 2004] does not explain the magnetic anomalies.

[4] Unusual geologic terranes have been identified on the Moon at locations antipodal to major impact basins. A unit of grooves and mounds has been mapped near Mare Ingenii in the region antipodal to Imbrium (Figure 2a). This unique geologic material is observed to cover craters and other terra of pre-Nectarian through Imbrian age, and appears to have formed nearly simultaneously during the Imbrian Period [*Stuart-Alexander*, 1978]. Suggested origins for this material include a concentration of basin ejecta from Imbrium [e.g., *Moore et al.*, 1974; *Stuart-Alexander*, 1978]

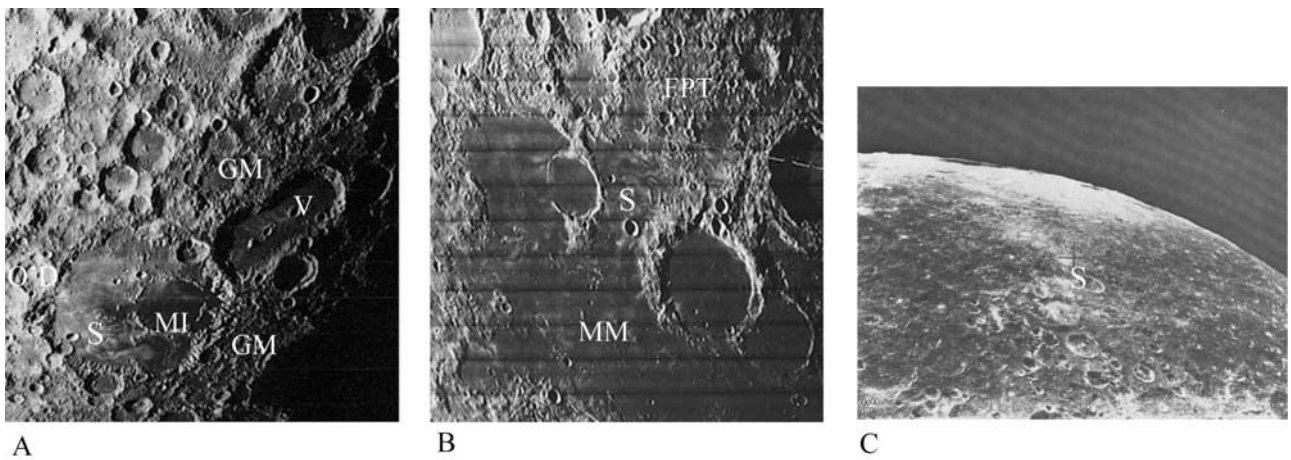

Figure 2. (a) Part of the area antipodal to Imbrium showing the high-albedo swirls (S) on Mare Ingenii (MI) and areas of grooves and mounds (GM). See Figure 5 for the detailed distribution of the GM unit. Other labeled features are O'Day (O'D, Copernican-aged crater) and Van de Graaff (V, cratering heavily modified by grooves and mounds and mare infill). From Lunar Orbiter II Frame 075 M. (b) Part of the region antipodal to the Orientale basin showing the high-albedo swirls (S) in the northern part of Mare Marginis (MM) and areas of the furrowed and pitted terrane (FPT). See Figure 3 for the detailed distribution of the FPT unit. From Lunar Orbiter IV Frame 165 H3. (c) The area antipodal to Crisium, showing high-albedo features (S) near the crater Gerasimovich. From Zond 8 photography.

or Serenitatis [*Wieczorek and Zuber*, 2001] and the convergence of seismic waves from Imbrium [e.g., *Schultz and Gault*, 1975; *Stuart-Alexander*, 1978]. Support for an ejecta origin is provided by Lunar Prospector gamma-ray data. It is widely believed that the crust of the Imbrium target was enriched in incompatible elements, including thorium [e.g., *Haskin*, 1998; *Korotev*, 2000]. *Lawrence et al.* [1998, 1999] have confirmed an enhancement of thorium antipodal to Imbrium, though *Wieczorek and Zuber* [2001] have suggested this may originate from Serenitatis ejecta.

[5] A furrowed and pitted terrane has been mapped antipodal to Orientale (Figure 2b). While ejecta [*Moore et al.*, 1974; *Wilhelms and El-Baz*, 1977] and seismic [*Schultz and Gault*, 1975] origins have been proposed for this terrane, the features are less sharply defined than those of the Imbrium antipode grooved terrane. The unit appears similar to the Descartes material from the Apollo 16 landing site [*Wilhelms and El-Baz*, 1977]. It is not clear that the two antipode terranes have a similar origin. However, if a seismic origin to these units is correct, the morphological differences may simply reflect different levels of consolidation at the antipodes at the time of the Orientale and Imbrium impacts. Alternatively, magnetometer and electron reflectometer data have shown a correlation between nearside anomalies and basin ejecta [e.g., *Strangway et al.*, 1973; *Anderson and Wilhelms*, 1979; *Halekas et al.*, 2001; *Richmond et al.*, 2003]. A previous study [*Hood and Williams*, 1989] has suggested a correlation between the two unusual antipode terranes and magnetic anomalies, which may support an ejecta origin to those terranes. Further, the similarities between the furrowed and pitted terrane and the Descartes material support an ejecta origin to the units. A magnetic anomaly has been shown to correlate with a high-albedo region of the Descartes Mountains [*Richmond et al.*, 2003] and it is generally agreed that the Descartes Mountains represent primary basin ejecta from Imbrium, Nectaris or both [e.g., *Spudis*, 1984].

[6] It has been suggested that there may be a small number of grooves antipodal to Serenitatis [e.g., *Hood and Williams*, 1989]. However, these may simply be secondary impacts related to nearby basins [*Wilhelms*, 1987]. There is not an extensive region of modified terrane as has been identified for Imbrium and Orientale. Due to the importance of solar phase angle on the albedo of the swirls [*Schultz and Srnka*, 1980], identification of swirls antipodal to Serenitatis is problematic due to limited photographic coverage at high solar phase angle. However, a number of swirls can be seen on Lunar Orbiter I Frame 38M.

[7] The fourth magnetic anomaly cluster is antipodal to Crisium and it includes the strongest anomaly currently mapped on the Moon. However, these anomalies are located near the Gerasimovich crater on the western edge of the Orientale ejecta sheet and any terrane in that area associated with the older Crisium impact will be buried beneath ejecta from Orientale. A group of swirls can be seen near Gerasimovich on a Zond 8 photograph obtained at high solar phase angle (Figure 2c).

[8] In this study, Lunar Prospector magnetometer data are used to carry out a correlation study between magnetic anomaly clusters antipodal to Imbrium, Orientale and Crisium, and the surface geology and swirls of those areas. Key aims are to identify possible source materials for the anomaly clusters and to address any correlations between the anomalies and swirls in these areas. The area antipodal to Serenitatis has not been considered due to limited magnetometer and photographic coverage. This study offers improvements over previous correlation work on these areas [*Hood and Williams*, 1989]. The magnetometer data obtained by Lunar Prospector is characterized by higher resolution as compared to the Apollo data which was used by *Hood and Williams* [1989]. Further, the near polar orbit of the Lunar Prospector spacecraft provides substantially better coverage than the Apollo subsatellite magnetometers which were in low inclination orbits. This provides improved coverage of the Imbrium and Crisium antipode areas.

2. Data Analysis and Correlation Results

[9] Low altitude (16–35 km) Lunar Prospector magnetometer data obtained during 1999 have been used. The data have been approximately continued to a constant elevation using an empirical inverse power law (see Appendix A). The areas of interest have been subdivided into 1° by 1° cells with each cell assigned two values: one describing the average magnetic field magnitude and the other the main geological unit within each cell. For each antipode area, the magnetic field strength has been subdivided into 1 nT bins. The number of 1° by 1° cells of each geologic terrane within each magnetic field strength bin have been counted. Occurrence rates have then been determined by dividing the number of cells of each geologic terrane in the bin by the total number of cells of that geologic type in the area. This was then carried out for all cells regardless of geology, to determine occurrence rates for the total number of cells within each magnetic field strength bin. Normalized occurrence rates were then determined by dividing the occurrence rates for each geologic terrane by the occurrence rates obtained when all cells were included. A normalized occurrence rate greater than 1 indicates a greater than average number of cells within a given field increment, while a value less than 1 indicates a lower than average correlation.

2.1. Orientale Antipode Anomalies

[10] Figure 3 is a superposition of a magnetic anomaly map of the Mare Marginis region of the Moon and the geologic map of *Wilhelms and El-Baz* [1977]. The data were obtained in June 1999 at an altitude varying from 16 to 24 km and have been upward continued to a constant altitude of 24 km. The geologic map of *Wilhelms and El-Baz* [1977] has been used to identify the terranes in each 1° by 1° cell. Terranes have been categorized as pre-Nectarian, Nectarian, furrowed and pitted terrane, young mare materials and others, where the latter includes all other geologic units and cells with a mixed surface geology. In all cases, each category is subdivided into the terrane with or without swirls.

[11] Normalized occurrence rates (Figure 4) indicate that most geologic units without swirls are characterized by low levels of magnetization. The furrowed and pitted terrane is the main exception to this, where a normalized occurrence rate of greater than 1 is obtained for field strengths in the range 5–6 nT. This implicates the furrowed and pitted terrane as a likely source. In contrast, all units with swirls

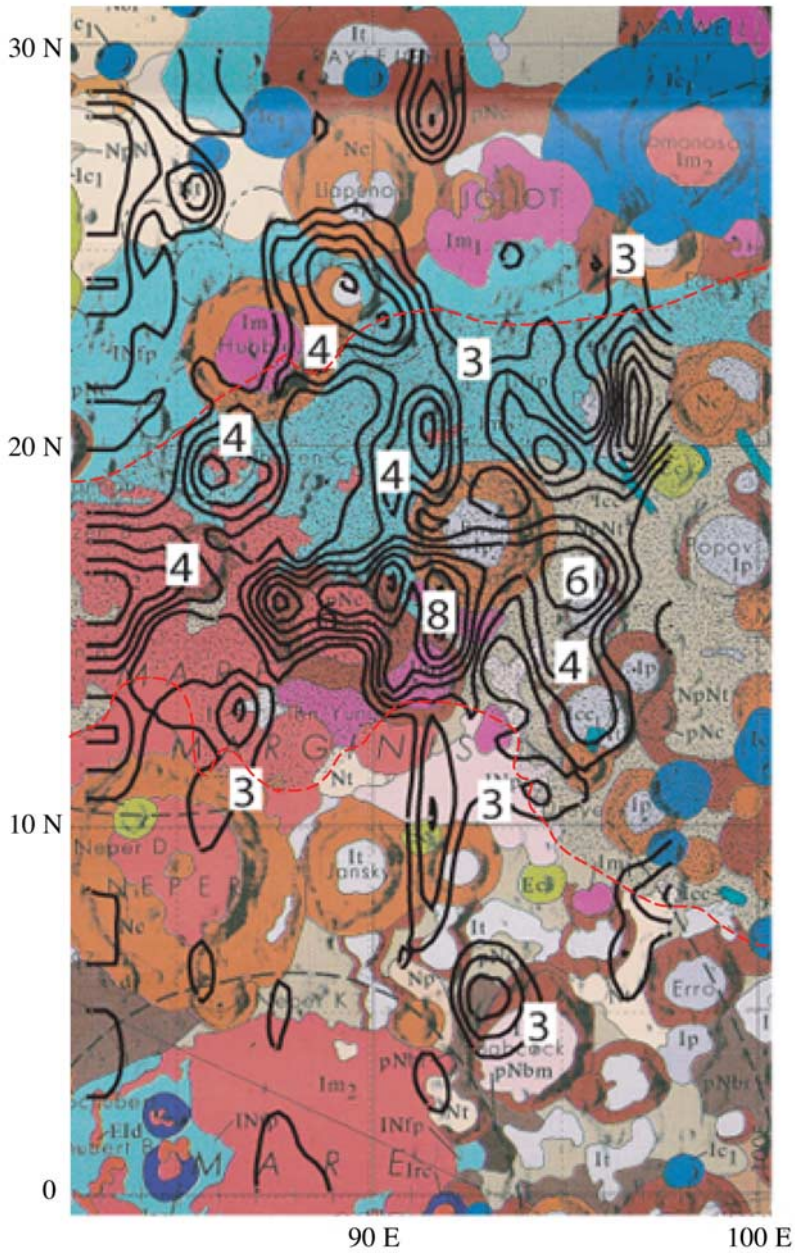

Figure 3. Magnetic field contour map of the Orientale antipode overlaying a geologic map of the area. The contour interval is 1 nT, starting at 3 nT. The geological map is from *Wilhelms and El-Baz* [1977]. The furrowed and pitted terrane is labeled INfp (the light blue unit across the upper half of the area). The region with high-albedo swirls is between the red dotted lines.

except the young mare materials show a correlation with areas of high crustal field strength. This is true for units that predate the Orientale impact (such as the pre-Nectarian terrane) as well as units believed to be of similar age or younger (furrowed and pitted terrane and others).

2.2. Imbrium Antipode Anomalies

[12] Magnetic field data obtained during April 1999, upward continued to 35 km as described in Appendix A, have been used (Figure 5). Geologic terranes have been identified from the geologic map of *Stuart-Alexander* [1978].

[13] Figure 6 is a plot of the normalized occurrence rates for the Imbrium antipode area and shows that Mare Ingenii materials both with and without swirls have a strong statistical correlation with regions of high magnetization. In general, the other mare materials are characterized by low field strength, with exceptions corresponding to small areas of mare surrounded by the grooved terrane northeast of Ingenii. The material of grooves and mounds shows a correlation with areas of high field strength, consistent with results obtained by *Hood and Williams* [1989]. Pre-Nectarian terranes have a normalized occurrence rate close to 1 in all cases, indicating a near average

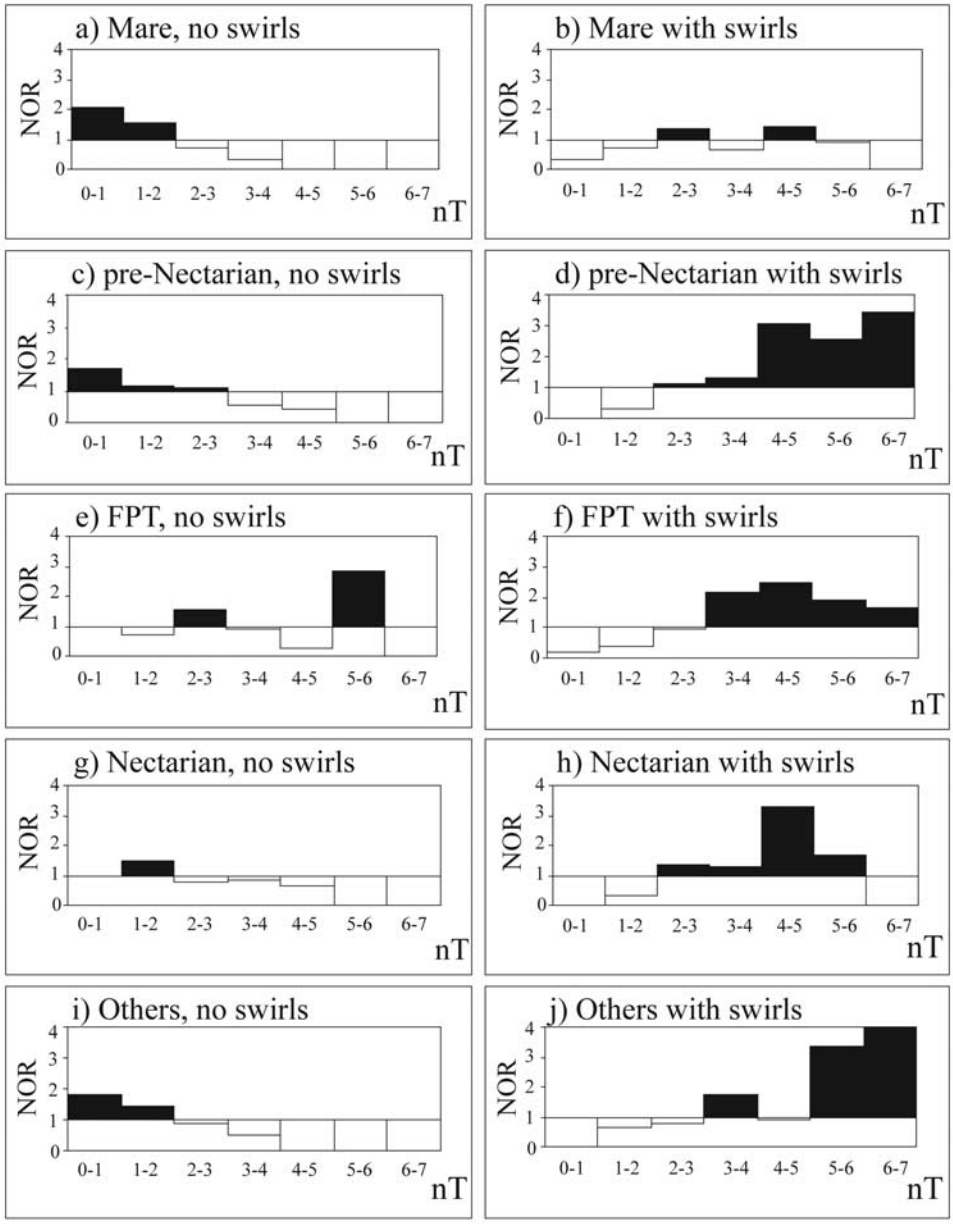

Figure 4. Normalized occurrence rates for the Orientale antipode, shown in black (for rates above 1) and white (for rates below 1). The normalizing factors used were 0.1 (0–1 nT), 0.37 (1–2 nT), 0.26 (2–3 nT), 0.14 (3–4 nT), 0.89 (4–5 nT), 0.04 (5–6 nT), and 0.01 (6–7 nT).

correlation with all magnetic field strengths. Craters of Imbrian age and younger show slight statistical correlations with areas of both low and high field strength. More detailed analysis has indicated that Imbrian and Eratosthenian aged craters are characterized by low field strengths, while Copernican aged cratering correlates with higher field strengths. With the exception of a few small Copernican aged impacts in the area, the only crater of that age is the 61 km O'Day crater (diameter from *Tompkins and Pieters* [1999]).

[14] The plains and terra materials of Nectarian and Imbrian age show a correlation with medium-high field strengths (Figure 6h). This group includes the Imbrian terra (It), light plains (INp) and smooth light plains (Ip) of *Stuart-Alexander* [1978]. These groups have been interpreted to be crater and/or basin ejecta associated with the formation of Imbrium, Nectaris and/or other similarly aged basins [*Stuart-Alexander*, 1978].

2.3. Crisium Antipode Anomalies

[15] Normalized occurrence rates have been determined for this area using magnetic field data obtained during July 1999, upward continued to a constant altitude of 24 km. The geology is taken from *Scott et al.* [1977] with swirl locations from *Hood and Williams*, 1989 (Figure 7). Due to the proximity of this anomaly cluster to the Orientale basin, only three terranes have been considered: Orientale ejecta (including the inner facies, outer facies and secondary cratering of the Helevius Formation), swirls and others, which includes all other terranes in the area.

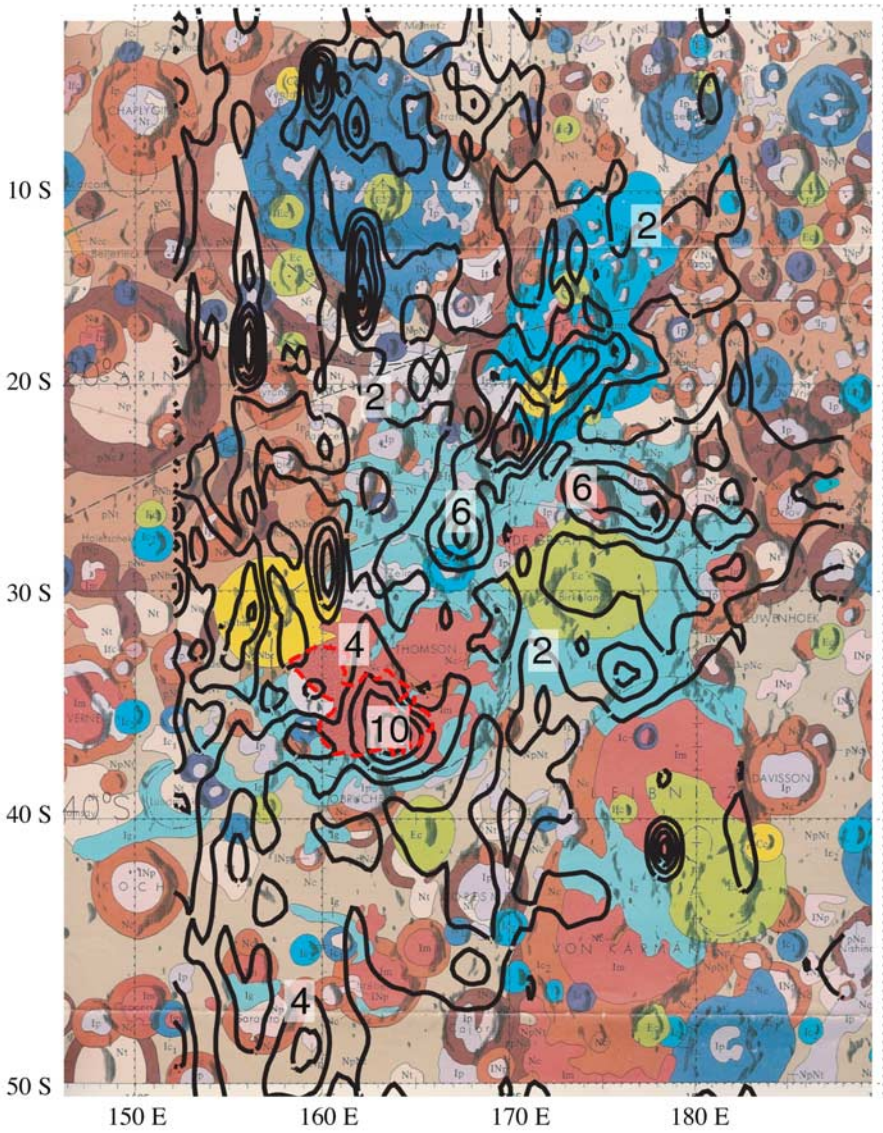

Figure 5. Magnetic field contour map of the Imbrium antipode overlaying a geologic map of the area. The contour interval is 2 nT, starting at 4 nT. The geologic map is from *Stuart-Alexander* [1978]. The material of grooves and mounds is labeled Ig (the light blue unit through the center of the map) and the high-albedo regions of Mare Ingenii are outlined in red.

[16] Normalized occurrence rates (Figure 8) show a strong statistical correlation between high-albedo swirls and regions of strong magnetization. In contrast, the other categories are characterized by low field strengths. The majority of swirls overlay Orientale ejecta units (~65%) with the remainder mostly of mixed surface geology (including ejecta units and Imbrian-aged craters).

3. Discussion

[17] The normalized occurrence rates presented here imply that high crustal fields are statistically correlated with the two antipode terranes and high-albedo swirl locations, consistent with the findings of *Hood and Williams* [1989]. With the exception of the proposed Serenitatis origin to the grooves near Mare Ingenii [*Wieczorek and Zuber*, 2001], these terranes are generally believed to be basin ejecta [e.g., *Moore et al.*, 1974] or seismically modified terrane [e.g., *Schultz and Gault*, 1975] associated with the antipodal basins.

[18] The location of the anomaly clusters antipodal to four similarly aged impact basins and the statistical correlation reported here argues for an association between Imbrian-aged basin forming impacts and crustal magnetic anomalies. In addition, Figure 6 suggests a correlation between Nectarian/Imbrian aged plains and terra and

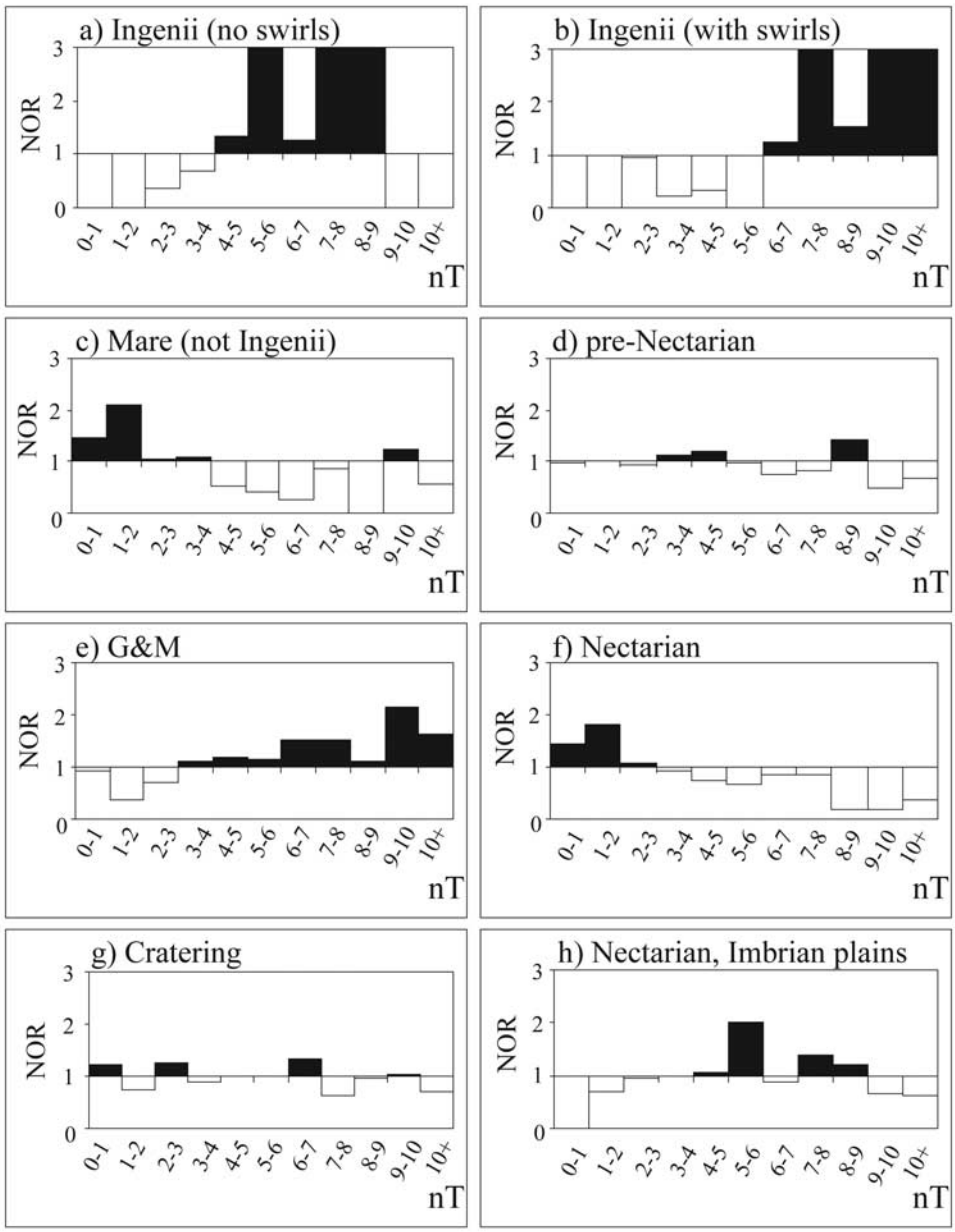

Figure 6. Normalized occurrence rates for the Imbrium antipode, shown in black (for rates above 1) and white (for rates below 1). Unless otherwise stated in the figure, all terranes are without swirls. The normalizing factors used were 0.19 (0–1 nT), 0.32 (1–2 nT), 0.22 (2–3 nT), 0.14 (3–4 nT), 0.07 (4–5 nT), 0.03 (5–6 nT), 0.02 (6–7 nT), and 0.01 (all other magnetic field strength bins).

medium-high crustal fields in the Mare Ingenii area. These units have been interpreted to be associated with the Imbrium and/or Nectaris basins [*Stuart-Alexander*, 1978]. These results offer further compelling evidence that strong lunar magnetic anomalies formed during the Imbrian Period. While we note that not all lunar magnetic anomalies are antipodal to Imbrian-aged basins, nearside anomalies such as the Descartes Mountains anomaly have been shown to correlate with basin ejecta units [e.g., *Richmond et al.*, 2003], a result consistent with returned sample data and surface measurements made at the Apollo landing sites [e.g., *Dyal et al.*, 1974]. In other cases, it has not been possible to identify the source of nearside anomalies. For example, the Reiner Gamma anomaly [*Hood*, 1980] is on the western edge of Oceanus Procellarum and the source is most likely to be buried below the mare materials.

[19] It would be highly coincidental for external events, such as cometary impacts, to occur in areas that are all antipodal to four similarly aged basins and to magnetize basin related terranes. Consequently, we believe these results provide further support for the plasma cloud model for the origin of the antipodal anomalies. In this model, a temporary, enhanced field is generated at the basin antipode as a result of an impact induced plasma cloud interacting with a weak field present at the Moon. The magnetization can then be acquired by shock remanence due to either

converging seismic waves or impacting basin ejecta. From the results reported here and a growing number of studies indicating that basin ejecta may be the source of the strong lunar anomalies, it may be inferred that the two antipode terranes are composed of basin ejecta.

[20] On the other hand, in the area near Mare Marginis, antipodal to Orientale, there is a statistical correlation between all geologic units and regions of medium to high field strength when swirls are present. This may offer support for a seismic component to the crustal fields, as all terranes that pre-date the antipodal impact would be affected. We also find that the O'Day crater antipodal to Imbrium correlates with medium-high levels of crustal magnetization. This 61 km crater is on the north east edge of Mare Ingenii, in an area dominated by the grooved

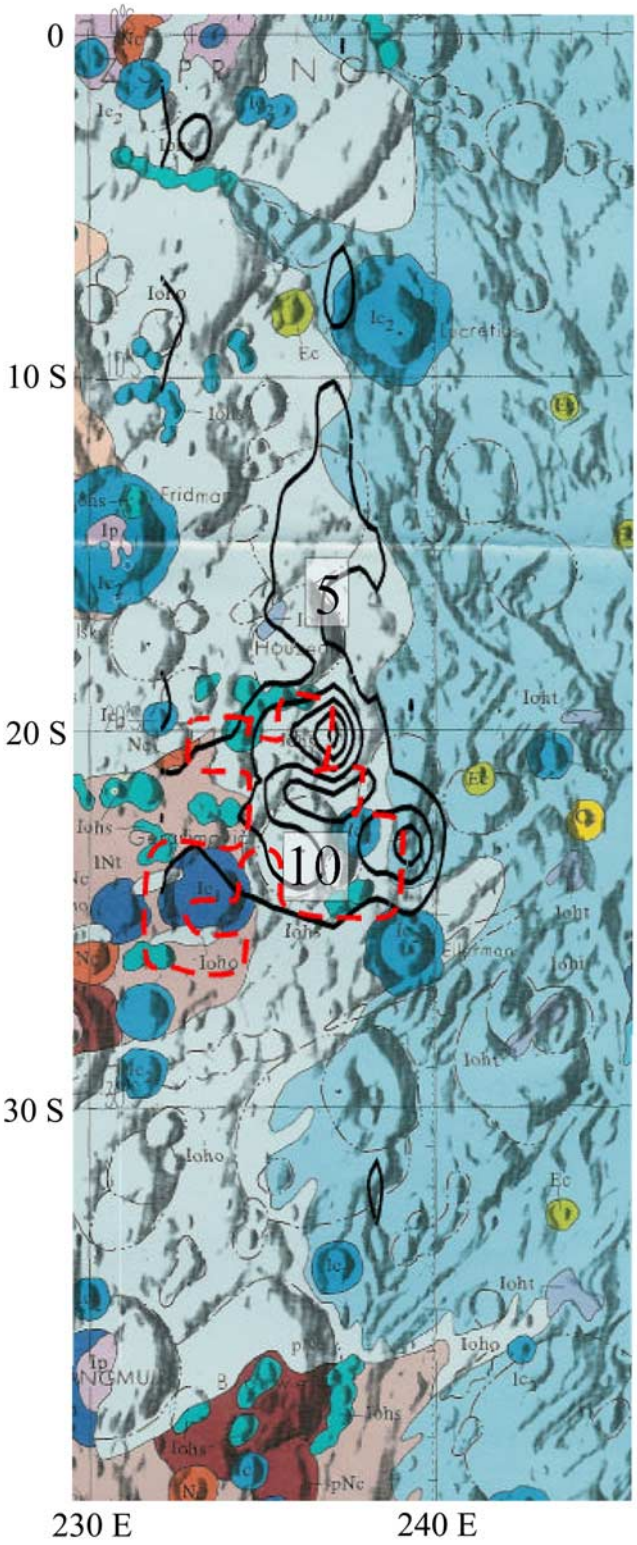

Figure 7. Magnetic field contour map of the Crisium antipode overlaying a geologic map of the area. The contour interval is 5 nT, starting at 5 nT. The geologic map is from *Scott et al.* [1977]. The location of the high-albedo features is outlined in red, taken from *Hood and Williams* [1989].

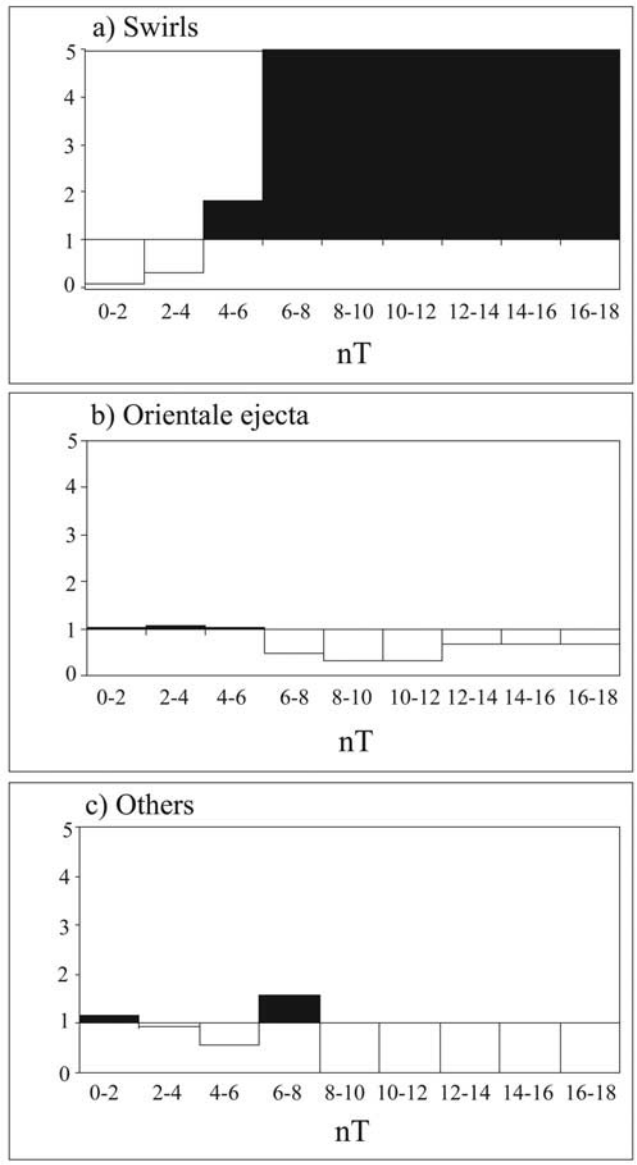

Figure 8. Normalized occurrence rates for the Crisium antipode, shown in black (for rates above 1) and white (for rates below 1). The normalizing factors used were 0.49 (0–1 nT), 0.33 (1–2 nT), 0.10 (2–3 nT), 0.04 (3–4 nT), 0.02 (4–5 nT), and 0.01 (all other magnetic field strength bins).

terrane. Previous work has indicated that full impact demagnetization occurs on the Moon for craters with diameters over approximately 50 km [*Halekas et al.*, 2002]. However, that was the resolution limit of that study and craters of smaller size may also be demagnetized. O'Day is larger than this size and it would be expected that it should be fully demagnetized if the anomaly source at that location is close to the surface. While we find that O'Day is of slightly lower field strength than the nearby grooved terrane, the lack of full demagnetization suggests that the source of the anomalies at O'Day may be relatively deep. It is noted that other cratering in the Imbrium antipode area are demagnetized, including Eratosthenian and Imbrian-aged craters. However, only two craters of a size comparable with O'Day have impacted close to the grooved terrane. It is possible that those impacts occurred in terrane that was not magnetized prior to impact or that the terrane was fully demagnetized by the slightly larger impacts. *Schultz and Gault* [1975] and others have found that seismic effects could extend to considerable depth below the antipodes and so the results presented here may suggest a seismic component to the remanent magnetization. However, there is strong evidence that basin ejecta are the most likely sources of lunar magnetic anomalies and there is currently insufficient evidence to differentiate between an ejecta or seismic origin.

[21] It is notable that other geologic terranes show a correlation with high field strengths in the areas antipodal to Imbrium and Orientale. The strongest correlation at the Imbrium antipode is for Mare Ingenii (both with and without swirls). This unit is more recent than the Imbrium impact and is located in an area dominated by the material of grooves and mounds (Figure 5). It is plausible that the source of the anomalies is the grooved terrane underlying the mare. Pre-Nectarian terranes show a near average statistical correlation with all field strengths antipodal to Imbrium. This is consistent with electron reflectometer data which have indicated that pre-Nectarian terranes are, at least in part, magnetized [*Halekas et al.*, 2001].

[22] In all cases, the strongest statistical correlation is shown between areas of high field strength and swirl locations. *Hood and Williams* [1989] noted that not all regions of magnetic field maxima coincided with swirl locations. However, the improved resolution provided by the Lunar Prospector magnetometer data suggests a strong statistical correlation between regions of high field strength and swirl locations for the Imbrium, Orientale and Crisium antipodes. This supports the correlation found for the Reiner Gamma anomaly [*Hood*, 1980] and the Descartes Mountains [*Richmond et al.*, 2003]. Combined with growing evidence for an Imbrian age to the magnetic anomalies, this supports a solar wind deflection origin to the lunar swirls. Alternate explanations for the swirls, including a cometary impact and meteoroid impact, propose that the swirls are young features. It would be highly fortuitous for recent surface scouring to occur in exactly the same areas as Imbrian aged magnetic anomalies. Micro-meteoroid impacts and solar wind ion bombardment have been proposed as likely external processes leading to optical maturation of lunar surface materials [e.g., *Housley*, 1977; *Pieters et al.*, 1993], but it has not yet been established whether ion bombardment is a necessary and/or significant component of the process [*Taylor et al.*, 2001]. We consider that the statistical correlations reported here may offer further evidence that the solar wind ion bombardment is a significant factor in the optical maturation of the lunar regolith.

[23] Finally, the data analyzed here unfortunately do not provide strong constraints on the existence and timing of a former lunar core dynamo. It should first be noted that the antipodal field amplification model [e.g., *Hood and Huang*, 1991] has not yet been developed in sufficient detail to either support or exclude the existence of a core dynamo when the magnetic anomalies in basin antipode zones were formed. This should be the subject of future work.

[24] The lack of significant crustal fields associated directly with the Imbrium and Orientale basins might initially be interpreted as implying that no core dynamo existed during the Imbrian epoch. However, paleointensity studies of returned samples [*Cisowski et al.*, 1983; *Fuller and Cisowski*, 1987] and electron reflectometer results for the Crisium basin [*Halekas et al.*, 2003] indicate otherwise. Also, unlike the Earth and Mars, the main ferromagnetic carriers on the Moon are metallic iron particles that are concentrated in impact generated ejecta materials. It is therefore uncertain whether sufficient ferromagnetic carriers were present in the deep resolidated crust beneath the basins to produce a significant magnetic anomaly.

[25] In both the Orientale and Imbrium antipode region, the results presented here indicate that Nectarian-aged terranes without swirls are magnetically weak suggesting the absence of a core dynamo during this epoch. However, this is not supported by electron reflectometer results [e.g., *Halekas et al.*, 2002]. In the Orientale antipode region, pre-Nectarian terranes without swirls are again magnetically weak. However, in the Imbrium antipode zone a near average statistical correlation is found for pre-Nectarian terranes with all field strengths. This is consistent with electron reflectometer data which have indicated that some pre-Nectarian terranes are associated with crustal magnetic fields. It is therefore not possible, on the basis of orbital data alone, to exclude the existence of a core dynamo during the pre-Nectarian epoch.

Appendix A

[26] Low-altitude (16–35 km) Lunar Prospector magnetometer data obtained during 1999 have been used. The method applied to produce the maps along the curved surface defined by the spacecraft altitude has been described in detail elsewhere [*Hood et al.*, 2001]. It can be summarized as follows. Initially, time intervals were selected when external field variations were minimized and data from those intervals were converted to a lunar radial, east and north coordinate system. Remaining low-frequency external field contributions were minimized by least squares fitting and removing a suitable polynomial function for each field component and each orbit. Finally, two dimensional filtering of the orbit data was carried out using a moving boxcar algorithm. The resulting data set was used to produce the vector magnetic field maps at variable spacecraft altitude.

[27] Constant altitude maps have been produced using an empirical inverse power law of the form

$$B_z = B_v / Z^x,$$

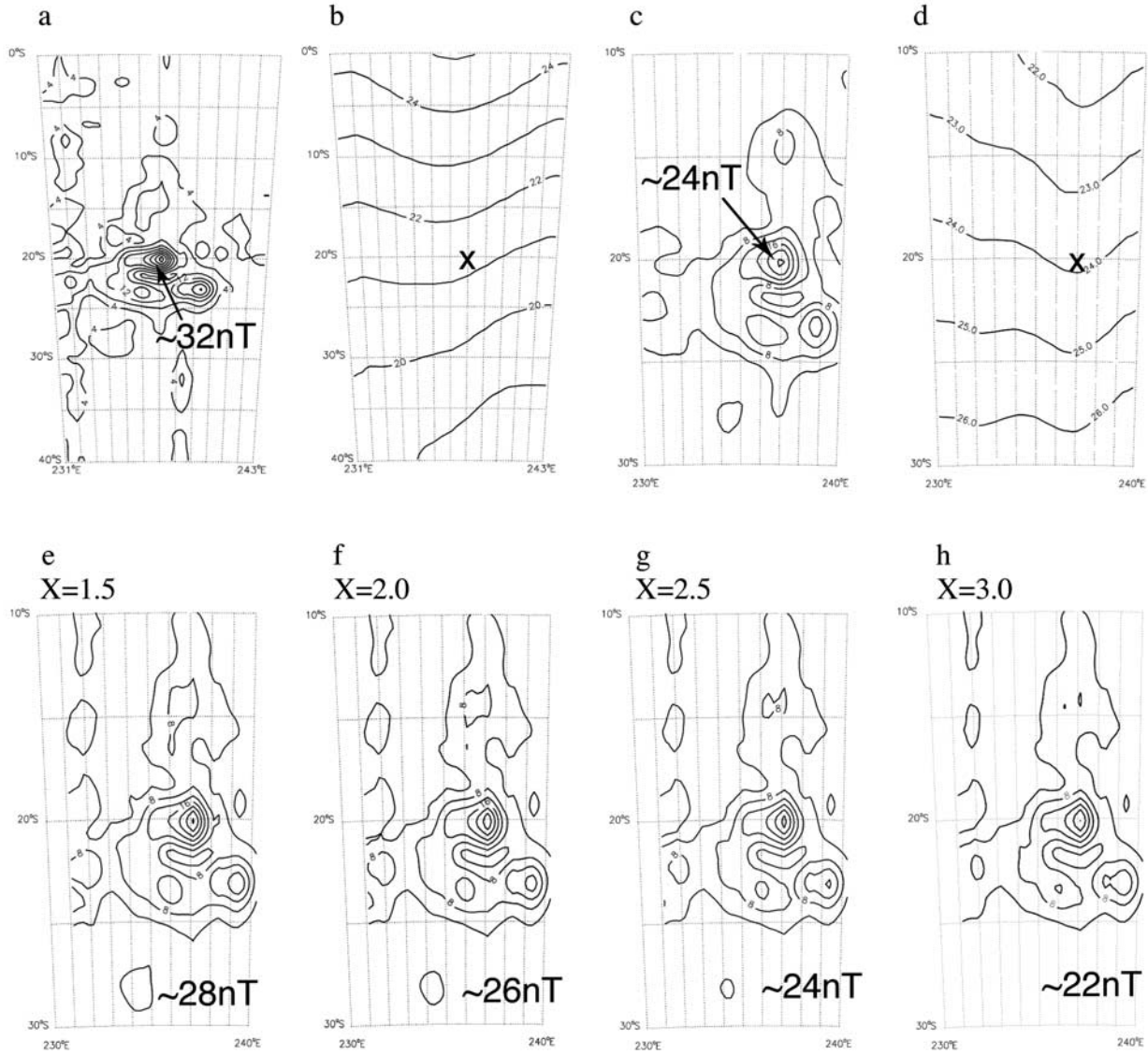

Figure A1. (a) Low-altitude magnetic field and (b) altitude contour maps of the Crisium antipode region. (c and d) The same area at higher altitude. The data in Figure A1a have been upward continued to the altitude of Figure A1c using different values of X (see text). Example output are given in Figures A1e–A1h. The values noted in Figures A1e–A1h correspond to the magnitude on each map at 20°S, 237°E which is at the altitude the low-altitude data (Figure A1a) were upward continued to for comparison with the high-altitude Lunar Prospector map (Figure A1c).

where B_z is the field at constant altitude Z, B_v is the field at variable spacecraft altitude and X is a site-specific constant. For the three areas of interest, maps have been identified providing coverage at two altitudes. The value of X has then been varied iteratively until the lower altitude map could be upward continued to the high altitude and provide field strengths consistent with the higher-altitude Lunar Prospector map.

[28] Figure A1 shows example output for the Crisium antipode. Low-altitude (18–25 km) coverage from July 1999 (Figures A1a and A1b) has been used to identify a strong anomaly located at 20°S, 237°E which has an amplitude of approximately 32 nT at 21.3 km altitude. The same anomaly was mapped in May 1999, with an amplitude of 24 nT at ~23.8 km (Figures A1c and A1d). The low-altitude map (Figure A1a) was upward continued to 23.8 km using different values of X. The anomaly magnitude at 20°S, 237°E on the upward continued map was compared with the magnitude at that location on the higher altitude Lunar Prospector map. The value of X was selected that yielded the closest agreement between the two maps at that specific location. Example output is presented in Figures A1e to A1h. For the Crisium antipode, the best fit was obtained for X = 2.5 (Figure A1g).

[29] This method has been applied to Imbrium and Orientale data to identify best fit values of X for those locations. For the Imbrium antipode, the best fit value was 1.2, while for the Orientale antipode it was 1.1. Using the

values of X determined in this way, variable altitude maps of the basin antipode areas have been upward continued to constant altitude. To minimize the distance each map has been continued over, the three areas have not been taken to the same altitude. Instead, each map has been continued to the lowest constant altitude possible for each area.

[30] **Acknowledgments.** Processing and mapping of the Lunar Prospector magnetometer data were supported by the NASA Lunar Data Analysis Program through a contract from the Lunar Research Institute. We thank Jafar Arkani-Hamed for useful discussions and Jasper Halekas and Erika Harnett for useful reviews.

References

Anderson, K. A., and D. E. Wilhelms (1979), Correlation of lunar farside magnetized regions with ringed impact basins, *Earth Planet. Sci. Lett.*, *46*, 107–112.

Cisowski, S. M., D. W. Collinson, S. K. Runcorn, A. Stephenson, and M. Fuller (1983), A review of lunar paleointensity data and implications for the origin of lunar paleomagnetism, *Proc. Lunar Planet. Sci. Conf. 13th*, Part 2, *J. Geophys. Res.*, *88*, suppl., A691–A704.

Crawford, D. A., and P. H. Schultz (1993), The production and evolution of impact-generated magnetic fields, *Int. J. Impact Eng.*, *14*, 205–216.

Crawford, D. A., and P. H. Schultz (1999), Electromagnetic properties of impact-generated plasma, vapour and debris, *Int. J. Impact Eng.*, *23*, 169–180.

Dyal, P., C. W. Parkin, and W. D. Daily (1974), Magnetism and the interior of the Moon, *Rev. Geophys.*, *12*, 568–591.

Fuller, M., and S. Cisowski (1987), Lunar paleomagnetism, in *Geomagnetism*, vol. 2, edited by J. Jacobs, pp. 307–456, Elsevier, New York.

Gold, T., and S. Soter (1976), Cometary impact and the magnetization of the Moon, *Planet. Space Sci.*, *24*, 45–54.

Halekas, J. S., D. L. Mitchell, R. P. Lin, S. Frey, L. L. Hood, M. H. Acuña, and A. B. Binder (2001), Mapping of crustal magnetic anomalies on the lunar near side by the Lunar Prospector electron reflectometer, *J. Geophys. Res.*, *106*, 27,841–27,852.

Halekas, J. S., D. L. Mitchell, R. P. Lin, L. L. Hood, M. H. Acuña, and A. B. Binder (2002), Demagnetization signatures of lunar impact craters, *Geophys. Res. Lett.*, *29*(13), 1645, doi:10.1029/2001GL013924.

Halekas, J. S., R. P. Lin, and D. L. Mitchell (2003), Magnetic fields of lunar multi-ring impact basins, *Meteorit. Planet. Sci.*, *38*, 565–578.

Harnett, E. M., and R. M. Winglee (2003), 2.5-D fluid simulations of the solar wind interacting with multiple dipoles on the surface of the Moon, *J. Geophys. Res.*, *108*(A2), 1088, doi:10.1029/2002JA009617.

Haskin, L. A. (1998), The Imbrium impact event and the thorium distribution at the lunar highlands surface, *J. Geophys. Res.*, *103*, 1679–1689.

Hood, L. L. (1980), Bulk magnetization properties of the Fra Mauro and Reiner Gamma formations, *Proc. Lunar Planet. Sci. Conf. 11th*, 1879–1896.

Hood, L. L. (1987), Magnetic field and remanent magnetization effects of basin-forming impacts on the Moon, *Geophys. Res. Lett.*, *14*, 844–847.

Hood, L. L., and Z. Huang (1991), Formation of magnetic anomalies antipodal to lunar impact basins: Two-dimensional model calculations, *J. Geophys. Res.*, *96*, 9837–9846.

Hood, L. L., and G. Schubert (1980), Lunar magnetic anomalies and surface optical properties, *Science*, *208*, 49–51.

Hood, L. L., and A. Vickery (1984), Magnetic field amplification and generation in hypervelocity meteoroid impacts with application to lunar paleomagnetism, *Proc. Lunar Planet. Sci. Conf. 15th*, Part 1, *J. Geophys. Res.*, *89*, suppl., C211–C223.

Hood, L. L., and C. R. Williams (1989), The lunar swirls: Distribution and possible origins, *Proc. Lunar Planet. Sci. Conf. 19th*, 99–113.

Hood, L. L., A. Zakharian, J. Halekas, D. L. Mitchell, R. P. Lin, M. H. Acuña, and A. B. Binder (2001), Initial mapping and interpretation of lunar crustal magnetic anomalies using lunar prospector magnetometer data, *J. Geophys. Res.*, *106*, 27,825–27,839.

Housley, R. M. (1977), Solar wind and micrometeorite effects in the lunar regolith, *Philos. Trans. R. Soc. London, Ser. A*, *285*, 363–370.

Korotev, R. L. (2000), The great lunar hot spot and the composition of and origin of the Apollo mafic ("LKFM") impact-melt breccias, *J. Geophys. Res.*, *105*, 4317–4345.

Lawrence, D. J., W. C. Feldman, B. L. Barraclough, A. B. Binder, R. C. Elphic, S. Maurice, and D. R. Thomsen (1998), Global elemental maps of the Moon: The Lunar Prospector gamma-ray spectrometer, *Science*, *281*, 1484–1489.

Lawrence, D. J., W. C. Feldman, B. L. Barraclough, A. B. Binder, R. C. Elphic, S. Maurice, M. C. Miller, and T. H. Prettyman (1999), High resolution measurements of absolute thorium abundances on the lunar surface, *Geophys. Res. Lett.*, *26*, 2681–2684.

Lin, R. P., K. A. Anderson, and L. L. Hood (1988), Lunar surface magnetic field concentrations antipodal to young large impact basins, *Icarus*, *74*, 529–541.

Lin, R. P., D. L. Mitchell, D. W. Curtis, K. A. Anderson, C. W. Carlson, J. McFadden, M. H. Acuña, L. L. Hood, and A. B. Binder (1998), Lunar surface magnetic fields and their interaction with the solar wind: Results from Lunar Prospector, *Science*, *281*, 1480–1484.

Moore, H. J., C. A. Hodges, and D. H. Scott (1974), Multiringed basins-illustrated by Orientale and associated features, *Geochim. Cosmochim. Acta*, *1*, suppl., 71–100.

Pieters, C., E. Fischer, O. Rode, and A. Basu (1993), Optical effects of space weathering: The role of the finest fraction, *J. Geophys. Res.*, *98*, 20,817–20,824.

Richmond, N. C., L. L. Hood, J. S. Halekas, D. L. Mitchell, R. P. Lin, M. H. Acuña, and A. B. Binder (2003), Correlation of a strong lunar magnetic anomaly with a high-albedo region of the Descartes mountains, *Geophys. Res. Lett.*, *30*(7), 1395, doi:10.1029/2003GL016938.

Schultz, P. H., and D. E. Gault (1975), Seismic effects from major basin formations on the Moon and Mercury, *Moon*, *12*, 159–177.

Schultz, P. H., and L. J. Srnka (1980), Cometary collisions with the Moon and Mercury, *Nature*, *284*, 22–26.

Scott, D. H., J. F. McCauley, and M. N. West (1977), Geologic map of the west side of the Moon, *U.S. Geol. Surv. Misc. Geol. Invest. Ser.*, *Map I-1034*.

Spudis, P. D. (1984), Apollo 16 site geology and impact melts: Implications for the geological history of the lunar highlands, *Proc. Lunar Planet. Sci. Conf. 15th*, Part 1, *J. Geophys. Res.*, *89*, suppl., C95–107.

Starukhina, L. V., and Y. G. Shkuratov (2004), Swirls on the Moon and Mercury: Meteoroid swarm encounters as a formation mechanism, *Icarus*, *167*, 13–147.

Strangway, D. W., H. Sharpe, W. Gose, and G. Pearce (1973), Lunar magnetic anomalies and the Cayley Formation, *Nature*, *246*, 112–114.

Stuart-Alexander, D. E. (1978), Geologic map of the central far side of the Moon, *U.S. Geol. Surv. Misc. Invest. Ser.*, *Map I-1047*.

Taylor, L. A., C. M. Pieters, L. P. Keller, R. V. Morris, and D. S. McKay (2001), Lunar mare soils: Space weathering and the major effects of surface-correlated nanophase Fe, *J. Geophys. Res.*, *106*, 27,985–27,999.

Tompkins, A., and C. M. Pieters (1999), Mineralogy of the lunar crust: Results from Clementine, *Meteorit. Planet. Sci.*, *34*, 25–41.

Wieczorek, M. A., and M. T. Zuber (2001), A Serenitatis origin for the Imbrium grooves and South Pole-Aitken thorium anomaly, *J. Geophys. Res.*, *106*, 27,853–27,864.

Wilhelms, D. E. (1987), The geologic history of the Moon, *U.S. Geol. Surv. Prof. Pap.*, *1348*.

Wilhelms, D., and F. El-Baz (1977), Geologic map of the east side of the Moon, *U.S. Geol. Surv. Misc. Geol. Invest. Ser.*, *Map I-948*.

M. H. Acuña, NASA Goddard Space Flight Center, Greenbelt, MD 20771, USA.

A. B. Binder, Lunar Research Institute, Tucson, AZ 85747, USA.

L. L. Hood, Lunar and Planetary Laboratory, University of Arizona, Tucson, AZ 85721, USA.

R. P. Lin and D. L. Mitchell, Space Science Laboratory, University of California, Berkeley, Berkeley, CA 94720, USA.

N. C. Richmond, Institute of Geophysics and Planetary Physics, Scripps Institution of Oceanography, University of California, San Diego, 9500 Gilman Drive, La Jolla, CA 92093, USA. (nic@ucsd.edu)